Received: 8 February 2018 | Revised: 9 April 2018 | Accepted: 29 August 2018

DOI: 10.1002/cta.2569

RESEARCH ARTICLE

WILEY

A symmetric pair of hyperchaotic attractors

Chunbiao Li[1,2] | Akif Akgul[3] | Julien Clinton Sprott[4] | Herbert H.C. Iu[5] | Wesley Joo-Chen Thio[6]

[1]Jiangsu Key Laboratory of Meteorological Observation and Information Processing, Nanjing University of Information Science and Technology, Nanjing 210044, China

[2]School of Electronic and Information Engineering, Nanjing University of Information Science and Technology, Nanjing 210044, China

[3]Faculty of Technology, Department of Electrical and Electronics Engineering, Sakarya University of Applied Sciences, Sakarya 54050, Turkey

[4]Department of Physics, University of Wisconsin—Madison, Madison, WI 53706, USA

[5]School of Electrical, Electronic, and Computing Engineering, The University of Western Australian, 35 Stirling Highway, Crawley, WA 6009, Australia

[6]Department of Electrical and Computer Engineering, The Ohio State University, Columbus, OH 43210, USA

Correspondence
Akif Akgul, Faculty of Technology, Department of Electrical and Electronics Engineering, Sakarya University of Applied Sciences, Sakarya 54050, Turkey.
Email: aakgul@sakarya.edu.tr; akifakgul@ieee.org

Funding information
Priority Academic Program Development of Jiangsu Higher Education Institutions; Sakarya University Scientific Research Projects Unit, Grant/Award Number: 2017-09-00-010; Startup Foundation for Introducing Talent of NUIST, Grant/Award Number: 2016205; Natural Science Foundation of the Higher Education Institutions of Jiangsu Province, Grant/Award Number: 16KJB120004

Summary

A symmetric pair of hyperchaotic attractors based on the 4-D Rössler system is constructed by adjusting the polarity information of some of its variables. By introducing a plane of equilibria into this system, an attractor and a repellor can be bridged. As a result, the proposed system is revised to be time-reversible, and one of the coexisting attractors can be extracted. Therefore, two coexisting hyperchaotic attractors can be captured separately in an electric circuit without an external circuit to set initial conditions, which has not been previously reported.

KEYWORDS

hyperchaotic attractor, hyperchaotic repellor, Rössler system, symmetric pair of coexisting attractors

1 | INTRODUCTION

Multistability has attracted great interest in the nonlinear research, and many coexisting attractors can be found in symmetric systems[1-14] and asymmetric systems.[15-20] Although a symmetric pair of coexisting strange attractors has been reported in a 3-D or 4-D system, the phenomenon of coexisting symmetric pair of hyperchaotic attractors has not been previously reported. In a 4-D symmetric system,[13,14] the coexisting symmetric pair of strange attractors usually merge together before turning into a single hyperchaotic attractor. Many hyperchaotic systems have been designed using extensions of the Lorenz and Rössler systems,[21-28] where most of the polynomial nonlinearities are based on quadratic nonlinearities without exhibiting coexisting hyperchaos. System coupling[29-31] and the time-delayed state feedback[32] can be applied for generating hyperchaos while desired higher-dimensional dissipative hyperchaotic systems can be constructed by using a single-parameter controller.[33] Unlike the above methods, and rather than increasing the degree of the nonlinear terms, such as cubic[26,34] or quintic nonlinearities,[35] we instead modulate the polarity information of some variables in a dynamical system. As a result, the asymmetric hyperchaotic Rössler equation is revised to be a symmetric one, and it produces a symmetric pair of hyperchaotic attractors.

In Section 2, a symmetric pair of hyperchaotic attractors is obtained by revising the structure of the hyperchaotic Rössler system. In Section 3, we discuss the relationship between the attractor and repellor and show a method to turn one of the coexisting attractors into a repellor. A circuit implementation for reproducing these coexisting attractors is discussed in Section 4, which agrees with the numerical simulation. The last section provides discussion and conclusions.

2 | COEXISTING HYPERCHAOTIC ATTRACTORS

The following four-dimensional Rössler equation.[21]

$$\begin{cases} \dot{x} = -y - z \\ \dot{y} = x + ay + u \\ \dot{z} = b + xz \\ \dot{u} = cu - dz \end{cases} \tag{1}$$

has a single asymmetric hyperchaotic attractor. Since the signal z is positive, we can revise the third dimension to be $\dot{z} = b\,\mathrm{sgn}(z) + x|z|$so as to construct a symmetric structure,

$$\begin{cases} \dot{x} = -y - z \\ \dot{y} = x + ay + u \\ \dot{z} = b\,\mathrm{sgn}(z) + x|z| \\ \dot{u} = cu - dz \end{cases} \tag{2}$$

There are discontinuous functions in the right-hand side, but according to the theorem shown in Davy,[36] here $F(t, \boldsymbol{V})$ is measurable and piecewise continuous according to the vector $\boldsymbol{V} = (x, y, z, u)$ and therefore system (2) has Filippov solution. System (2) has inversion symmetry with respect to the original point based on the invariance under the coordinate transformation $(x, y, z, u) \to (-x, -y, -z, -u)$, and hence it has a symmetric pair of coexisting attractors. When $a = 0.25$, $b = 3$, $c = 0.05$, and $d = 0.5$, and initial conditions are (0, 1, 3, 18), System (2) is hyperchaotic with Lyapunov exponents (LEs) of (0.1121, 0.0213, 0, −24.9268) and a Kaplan-Yorke dimension of $D_{\mathrm{KY}} = 3\text{-}(\lambda_1 + \lambda_2)/\lambda_4 \approx 3.0054$. As predicted, System (2) gives a symmetric pair of coexisting hyperchaotic attractors. Figure 1 shows various projections of the coexisting hyperchaotic attractors, which resemble the attractor for System (1). The cross section of the attractor in the hyperchaotic region shown in Figure 2 has a dimension greater than 2.0, indicating that the capacity dimension of the attractor is greater than 3.0.

When considering the nonlinear feedback in the hyperchaotic equations, all nonlinearities come from the third dimension of z. Variable z can be replaced with an absolute-value term $|z|$, and its polarity can be preserved by sgn (z). Consequently, these substitutions can preserve the hyperchaos in the symmetric space. Correspondingly, the symmetric system (2) has symmetric equilibrium points. When $a = 0.25$, $b = 3$, $c = 0.05$, and $d = 0.5$, the system has three equilibrium points: one at the origin (0, 0, 0, 0) with eigenvalues (0, 0.05, $0.125 \pm 0.9922i$), which is an unstable

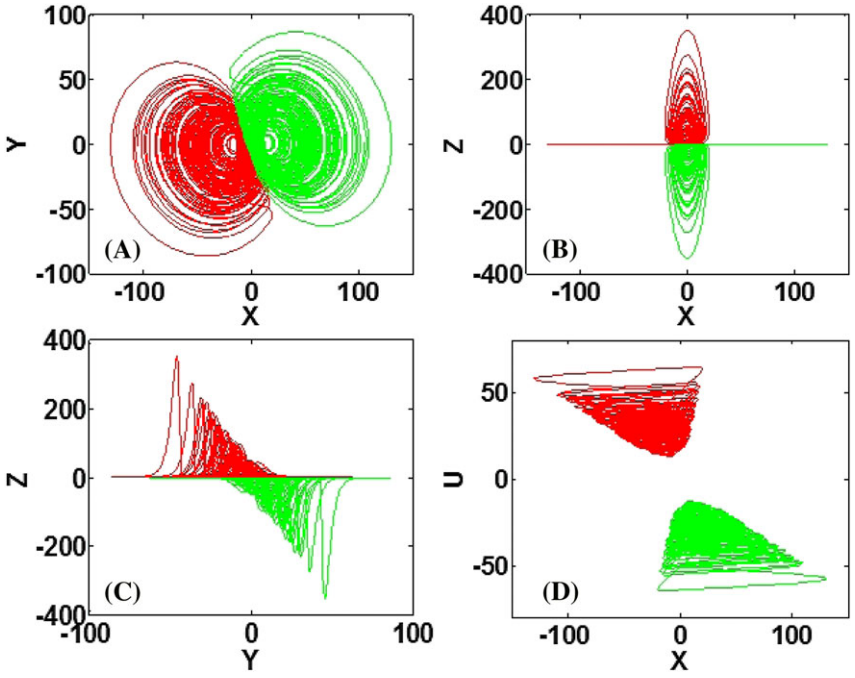

FIGURE 1 Projections of coexisting hyperchaotic attractors of system (2) for a = 0.25, b = 3 and c = 0.05, d = 0.5. A, x-y phase plane; B, x-z phase plane; C, y-z phase plane; D, x-u phase plane, red for (−6,0, 0.5, 14) and green for (6,0, −0.5, −14) [Colour figure can be viewed at wileyonlinelibrary.com]

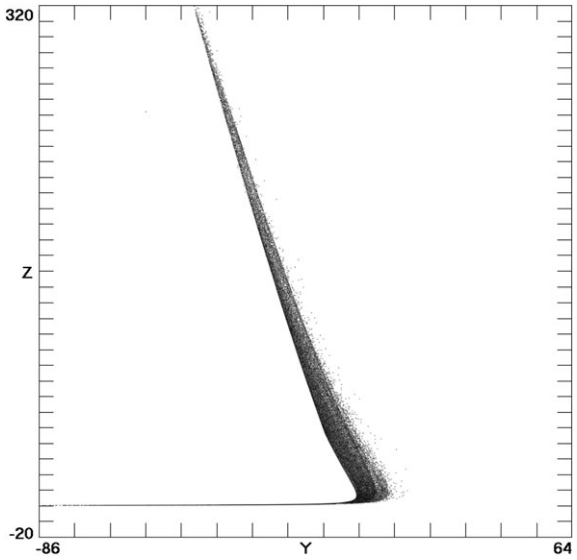

FIGURE 2 Projection onto the y-z plane of a cross section of the hyperchaotic attractor at x = 0, u = 0 for system (2) with a = 0.25, b = 3, c = 0.05, and d = 0.5

node; and two other equilibrium points at (±5.4083, ±0.5547, ∓0.5547, ∓5.5470) with eigenvalues (−5.3090, 0.1019, 0.0494 ± 0.9987i), which are four-dimensional saddle-foci. This indicates that the coexisting attractors are self-excited rather than hidden.[14,34,37-41]

Here, our computation of LEs is based on the algorithm of Wolf rather from Kuznetsov,[42] which is also a finite-time LE, and the time is 4e7. Like other systems with signum functions, the discontinuous signum function causes difficulty in calculation of the LEs.[43,44] We avoided this difficulty by replacing sgn (*x*) with tanh (*Nx*) and choosing $N = 100$, which is sufficiently large that the calculated exponents are independent of its value to high precision. And consequently, the absolute value function can be smoothed by replacing with tanh (*Nx*)**x* since |*x*| = sgn (*x*)**x*. The initial conditions that were used here is (−6, 0, 0.5, 14) and other selected initial conditions give the same LEs to four significant digits.

3 | TURNING AN ATTRACTOR INTO A REPELLOR

To extract any of the coexisting attractors, a proper initial condition is necessary to produce the desired oscillation. However, by changing one of the coexisting attractors into a repellor, a circuit may be used to implement the remaining attractor from noise without needing a preselected initial condition. This can be done by revising the symmetric system to be a time-reversible system, which allows one of the coexisting attractors to become a repellor.[45-47] As shown in Figure 3, an odd function can bridge these two classes of systems, providing a new method to extract any of the symmetric attractors.

Theorem 1. *A super-plane of equilibria can be introduced into System (2) through* p = ± *sgn (z), which results in the following time-reversible system with inversion-invariant symmetry.*

$$\begin{cases} \dot{x} = (-y - z)p \\ \dot{y} = (x + ay + u)p \\ \dot{z} = (b\,\mathrm{sgn}(z) + x|z|)p \\ \dot{u} = (cu - dz)p \end{cases} \tag{3}$$

Proof. As pointed out in the first section, System (2) has inversion invariant symmetry, while the System (3) has a super-plane of equilibria at $z = 0$ when $p = \pm$ sgn (z). By making a transformation $(x, y, z, t) \rightarrow (-x, -y, -z, -t)$, System (3) will recover its original governing equation. Therefore, System (3) is time-reversible with inversion-invariant symmetry. The attractors and corresponding repellors with different functions are shown in Figure 4. The symmetric version can be restored by multiplying the same odd function since $\mathrm{sgn}(z) \times$ sgn $(z) = 1$. For further reading, see Li and Sprott.46 Here, in this paper, a simpler circuit structure is obtained by turning a symmetry system to a time-reversible one. From this operation, one of the coexisting attractors turns to be a repellor, and therefore it is more convenient to pick up the rest of

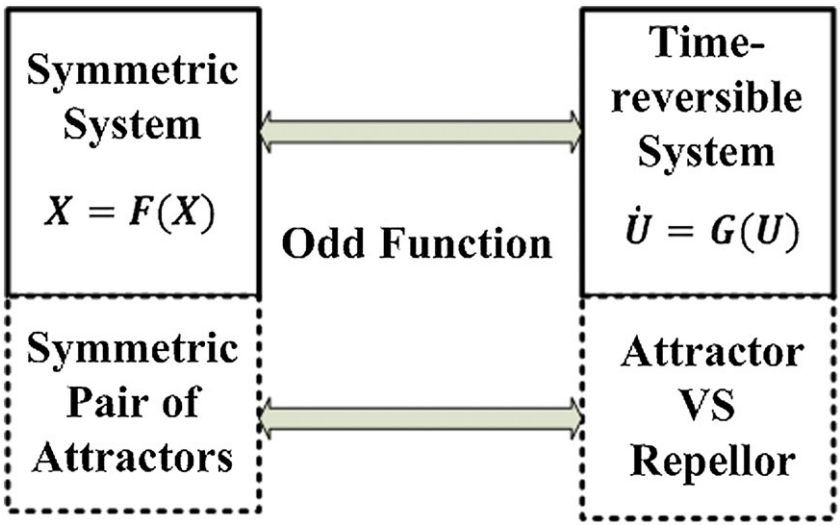

FIGURE 3 A bridge between the symmetric system and time-reversible system [Colour figure can be viewed at wileyonlinelibrary.com]

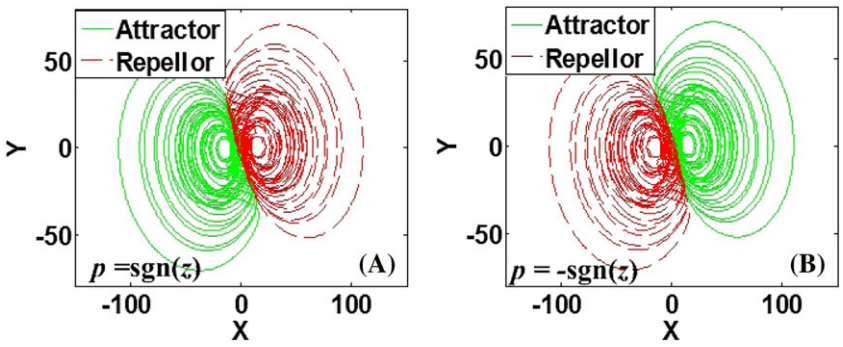

FIGURE 4 Selecting different attractors by introducing different functions p = ± sgn (z) [Colour figure can be viewed at wileyonlinelibrary.com]

coexisting attractors without needing an initial condition unit (ICU). In addition, the specific nonlinearity of signum function and absolute value function disappeared and can be replaced with switch operations.

System (2) does not have a hyperchaotic repellor. When time is reversed, the only attractor is the equilibrium at the origin (plus the one at infinity). In contrast, System (3) has a hyperchaotic repellor. Now, one of the coexisting hyperchaotic attractors is an invisible repellor (shown in red) and cannot be accessed regardless of the initial conditions, while the remaining attractor (shown in green) can be extracted for any accessible initial conditions. This can be accessed in an electronic circuit through inherent circuit noise.[48] In fact, the newly introduced odd function can be multiplied into each term, and if $p = \text{sgn}(z)$, System (3) can be rewritten as

$$\begin{cases} \dot{x} = -y\,\text{sgn}(z) - |z| \\ \dot{y} = x\,\text{sgn}(z) + ay\,\text{sgn}(z) + u\,\text{sgn}(z) \\ \dot{z} = b + xz \\ \dot{u} = cu\,\text{sgn}(z) - d|z| \end{cases}. \tag{4}$$

System (4) does not change its time-reversible property and only produces the desired attractor as shown in green in Figure 4A. In fact, when considering the attractor location in the space of $z > 0$, System (4) is equivalent to the original System (1). Following the same analysis, when $p = -\text{sgn}(z)$ System (3) becomes

$$\begin{cases} \dot{x} = -y - z \\ \dot{y} = x + ay + u \\ \dot{z} = -b - xz \\ \dot{u} = cu - dz \end{cases}. \tag{5}$$

The only difference between Systems (1) and (5) is the third dimension, which is $\dot{z} = \pm b \pm xz$. The attractor and the repellor exchange roles when System (1) switches to System (5), which is convenient for showing the symmetric pair of attractors in System (2).

4 | CIRCUIT REALIZATION

4.1 | A circuit implementation with initial conditions for attractor selection

The traditional method for reproducing coexisting attractors requires presetting the initial conditions. From Equation 2, we design the analog circuit shown in Figure 5 to generate the hyperchaotic attractors, which includes four channels to realize the integration, addition, and subtraction of the state variables x, y, z, and u, respectively. According to Kirchhoff's circuit laws and the property of the circuit elements, the equations in terms of the circuit parameters are

$$\begin{cases} \dot{x} = -\dfrac{1}{R_1C_1}y - \dfrac{1}{R_2C_1}z \\ \dot{y} = \dfrac{1}{R_3C_2}x + \dfrac{1}{R_4C_2}y + \dfrac{1}{R_5C_2}u \\ \dot{z} = \dfrac{1}{R_6C_3}\text{sgn}(z) + \dfrac{1}{R_7C_3}x|z| \\ \dot{u} = \dfrac{1}{R_8C_4}u - \dfrac{1}{R_9C_4}z \end{cases}. \tag{6}$$

The circuit includes an ICU for presetting suitable voltages on the capacitors C_1 to C_4. Typically, an electronic switch can fulfill this task. For example, the 0.45-Ω quad SPDT analog switch TS3A44159 can be used to realize initial condition presetting. As shown in the ICU in Figure 6, the control pin IN can be set to different voltages by the button (high level or low level determined by the voltage divider Rm and Rn). This allows for COM_i to either connect to NC_i (charging the capacitors through resistors R_{ih} and R_{ig}) or connect to NO_i and provides feedback to the oscillator.

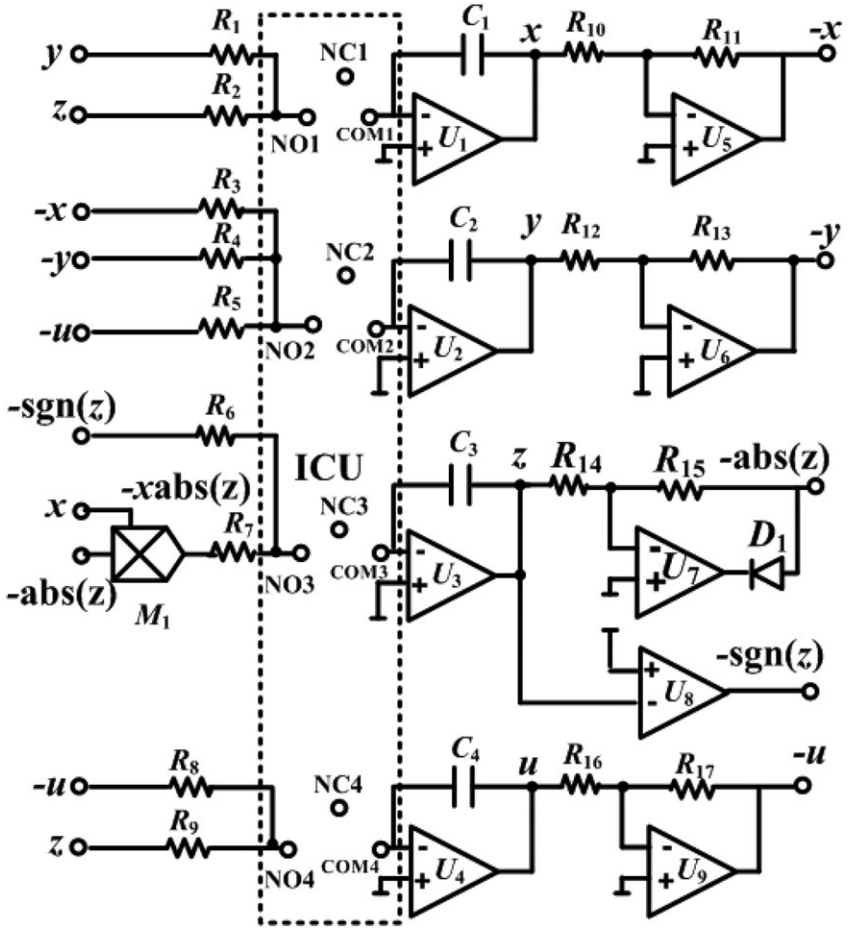

FIGURE 5 Four integration channels in circuit for the 4-D system (2)

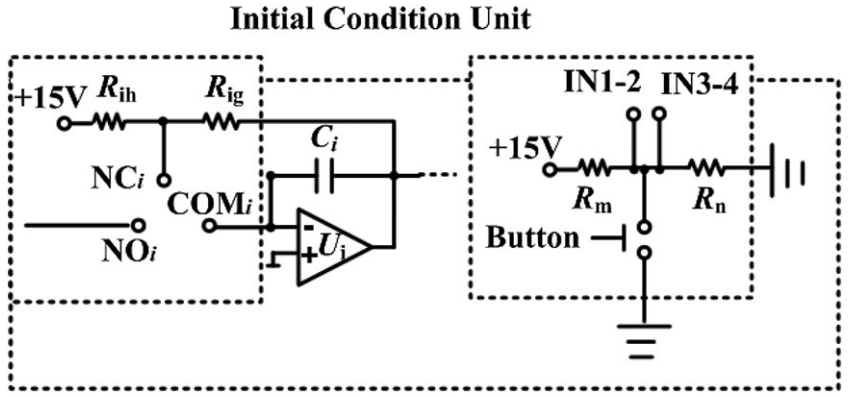

FIGURE 6 Initial condition unit for presetting the voltage on the capacitors

4.2 | Circuit constructing for reproducing attractors

However, the abovementioned circuit is complicated since it requires special circuit elements for the implementation of the absolute value, signum nonlinearity, and the ICU. When considering the relation between a symmetric system and a time-reversible one, usually four extra multipliers are required for realizing System (3). Fortunately, the circuit for representing the coexisting attractors can be simplified further based on Equations 1 and 5. As shown in Figure 7, through the general method of analog computation, four integration channels incorporated with the switch between $\mp V_{dd}$ and $\mp xz$ can be used to capture two coexisting hyperchaotic attractors separately. Here, the circuit schematic is really simplified. Compared with Figure 5, except the ICU there are also no circuit units for realizing the absolute value and signum nonlinearity in Figure 7. Figure 5 is designed to observe two coexisting attractors shown in Figure 1, while Figure 7 is constructed for catching one of the coexisting attractors separately shown as Figure 4. The circuit equations, where variables x, y, z, and u represent voltage levels, are given by

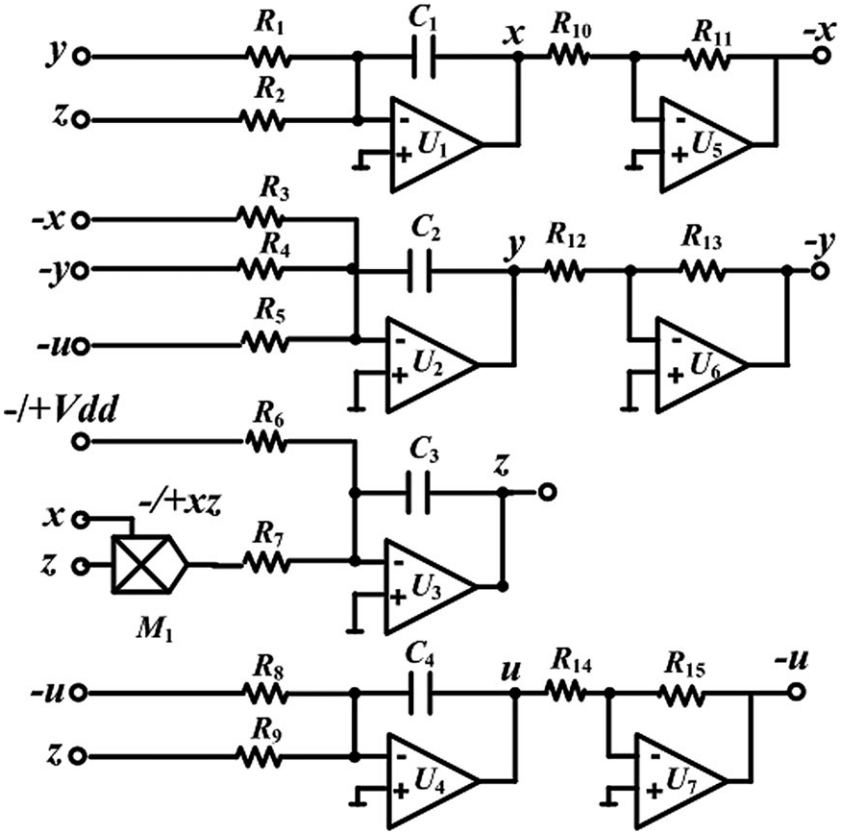

FIGURE 7 An equal schematic for switching the coexisting attractors

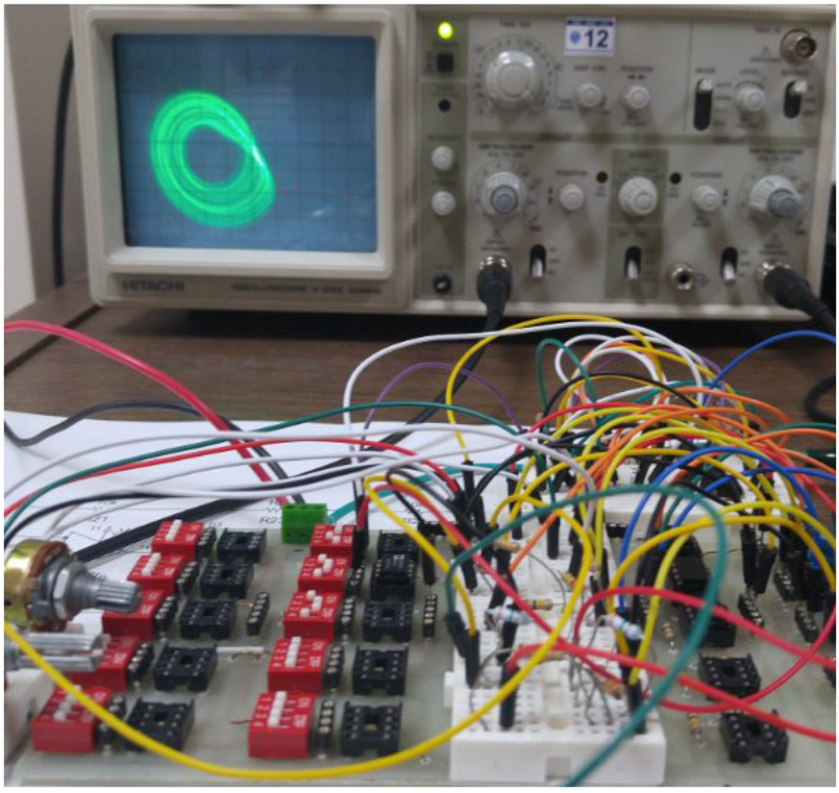

FIGURE 8 The experimental circuit in operation. The oscilloscope displays one of the coexisting hyperchaotic attractors [Colour figure can be viewed at wileyonlinelibrary.com]

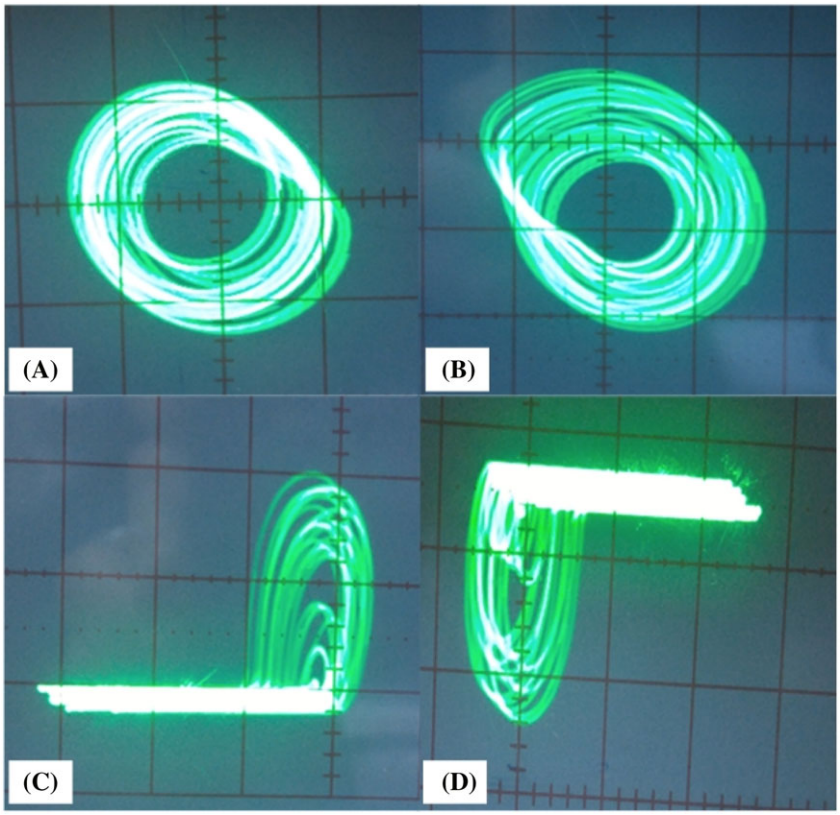

FIGURE 9 Oscilloscope traces of hyperchaotic attractors of system (2) A, and B, x-y plane, C, and D, x-z plane (1 V/div) [Colour figure can be viewed at wileyonlinelibrary.com]

$$\begin{cases} \dot{x} = -\dfrac{1}{R_1C_1}y - \dfrac{1}{R_2C_1}z \\ \dot{y} = \dfrac{1}{R_3C_2}x + \dfrac{1}{R_4C_2}y + \dfrac{1}{R_5C_2}u \\ \dot{z} = \pm\dfrac{Vdd}{R_6C_3} \pm \dfrac{1}{R_7C_3}xz \\ \dot{u} = \dfrac{1}{R_8C_4}u - \dfrac{1}{R_9C_4}z \end{cases}. \tag{7}$$

To avoid saturating analog multipliers and operational amplifiers, the system is rescaled as $x \to 20x$, $y \to 20y$, $z \to 40z$, $u \to 20u$, with circuit parameters: $R_1 = R_3 = R_5 = R_9 = 400$ kΩ, $R_2 = 200$ kΩ, $R_4 = 1.6$ MΩ, $R_6 = 1.06$ MΩ, $R_7 = 20$ kΩ, $R_8 = 8$ MΩ, $R_{10} = R_{11} = R_{12} = R_{13} = 20$ kΩ. The operational amplifiers are TL084 ICs powered by ±9 volts, and the constant branch V_{dd} is powered by ±5 volts. Several design considerations were taken into account to prevent degrading the hyperchaotic behavior. The experimental circuit in operation is shown in Figure 8. Oscilloscope traces from the output of the integration channels are given in Figure 9. Aside from a few transients originating from different initial conditions, the result is in agreement with Figure 1.

5 | CONCLUSION AND DISCUSSIONS

Hyperchaotic signals have great instability in two dimensions and relatively more complicated dynamics, and because of this, hyperchaotic circuits can improve security and carrier performance by providing pseudo-random signals that are useful in secure communications and radar engineering.[49-52] In this paper, a hyperchaotic system with a symmetric pair of coexisting attractors is proposed by constructing a symmetric structure and revising the polarity. The introduction of a signum function and absolute value function produces a polarity balance leading to a desired symmetric structure that does not destroy the dynamics of the original four-dimensional hyperchaotic Rössler system.

However, the corresponding circuit requires special elements to execute the specific nonlinearity and preset the initial conditions. A deeper examination of the relation between the symmetric system and the time-reversible system suggests that one of the coexisting attractors can be transformed into a repellor, and consequently the remaining attractor can be extracted by the inherent noise in the circuit without the need for an ICU. The simplified structure of the analog circuit designed in this paper reproduces the coexisting attractors separately without any complicated elements for realizing polarity transformation. The corresponding hyperchaotic attractors show good agreement with numerical simulation.

ACKNOWLEDGMENTS

This work was supported financially by the Natural Science Foundation of the Higher Education Institutions of Jiangsu Province (Grant No.:16KJB120004), the Startup Foundation for Introducing Talent of NUIST (Grant No.: 2016205), Sakarya University Scientific Research Projects Unit (Grants No.: 2017-09-00-010), and a Project Funded by the Priority Academic Program Development of Jiangsu Higher Education Institutions.

ORCID

Chunbiao Li http://orcid.org/0000-0002-9932-0914
Akif Akgul http://orcid.org/0000-0001-9151-3052
Julien Clinton Sprott http://orcid.org/0000-0001-7014-3283
Herbert H.C. Iu http://orcid.org/0000-0002-0687-4038

REFERENCES

1. Bao B, Li Q, Wang N, Xu Q. Multistability in Chua's circuit with two stable node-foci. *Chaos*. 2016;26(4). 043111
2. Xu Q, Lin Y, Bao B, Chen M. Multiple attractors in a non-ideal active voltage-controlled memristor based Chua's circuit. *Chaos Soliton Fract.* 2016;83:186-200.
3. Li C, Sprott JC. Multistability in the Lorenz system: a broken butterfly. *Int J Bifurcation Chaos*. 2014;24(10):1450131.
4. Li C, Hu W, Sprott JC, Wang X. Multistability in symmetric chaotic systems. *Eur Phys J Spec Top*. 2015;224(8):1493-1506.
5. Li C, Sprott JC, Yuan Z, Li H. Constructing chaotic systems with total amplitude control. *Int J Bifurcation Chaos*. 2015;25(10):1530025.
6. Li C, Sprott JC, Thio W. Linearization of the Lorenz system. *Phys Lett A*. 2015;379(10–11):888-893.
7. Lai Q, Chen S. Research on a new 3D autonomous chaotic system with coexisting attractors. *Optik*. 2016;127(5):3000-3004.
8. Lai Q, Chen S. Coexisting attractors generated from a new 4D smooth chaotic system. *Int J Control Autom*. 2016;14(4):1124-1131.
9. Kengne J, Njitacke ZT, Fotsin HB. Dynamical analysis of a simple autonomous jerk system with multiple attractors. *Nonlinear Dyn.* 2016;83(1–2):751-765.
10. Kengne J, Njitacke ZT, Nguomkam NA, Fouodji TM, Fotsin HB. Coexistence of multiple attractors and crisis route to chaos in a novel chaotic jerk circuit. *Int J Bifurcation Chaos*. 2016;26(05). 1650081
11. Li C, Sprott JC. Crisis in amplitude control hides in multistability. *Int J Bifurcation Chaos*. 2016;26(14). 1650233
12. Sprott JC. Simplest chaotic flows with involutional symmetries. *Int J Bifurcation Chaos*. 2014;24(1). 1450009
13. Li C, Sprott JC, Thio W. Bistability in a hyperchaotic system with a line equilibrium. *J Exp Theor Phys*. 2014;118(3):494-500.
14. Li C,Sprott JC. Coexisting hidden attractors in a 4-D simplified Lorenz system. *Int J Bifurcation Chaos*. 2014;24(3). 1450034
15. Sprott JC. A dynamical system with a strange attractor and invariant tori. *Phys Lett A*. 2014;378(20):1361-1363.
16. Barrio R, Blesa F, Serrano S. Qualitative analysis of the Rössler equations: bifurcations of limit cycles and chaotic attractors. *Physica D*. 2009;238(13):1087-1100.
17. Sprott JC, Wang X, Chen G. Coexistence of point, periodic and strange attractors. *Int J Bifurcation Chaos*. 2013;23(5):1350093.
18. Li C, Sprott JC, Xing H. Hypogenetic chaotic jerk flows. *Phys Lett A*. 2016;380(11–12):1172-1177.
19. Li C, Sprott JC. Variable-boostable chaotic flows. *Optik*. 2016;127(22):10389-10398.
20. Sprott JC, Li C. Asymmetric bistability in the Rössler system. *Acta Phys Pol B*. 2017;48(1):97-107.
21. Rössler OE. An equation for hyperchaos. *Phys Lett A*. 1979;71(2–3):155-157.
22. Ruy B. Dynamics of a hyperchaotic Lorenz system. *Int J Bifurcation Chaos*. 2007;17(12):4285-4294.
23. Qi G, Van Wyk MA, Van Wyk BJ, Chen G. On a new hyperchaotic system. *Phys Lett A*. 2008;372(2):124-136.

24. Wang Z, Cang S, Ochola EO, Sun Y. A hyperchaotic system without equilibrium. *Nonlinear Dyn*. 2012;69(1–2):531-537.
25. Li Y, Chen G, Wallace KST. Controlling a unified chaotic system to hyperchaotic. *IEEE Trans. on Circuits Syst.—II: Exp. Briefs*. 2005;52(4):204-207.
26. Li Q, Hu S, Tang S, Zeng G. Hyperchaos and horseshoe in a 4D memristive system with a line of equilibria and its implementation. *Int J Circ Theor Appl*. 2014;42(11):1172-1188.
27. Li Y, Tang WKS, Chen G. Hyperchaos evolved from the generalized Lorenz equation. *Int J Circ Theor Appl*. 2005;33(4):235-251.
28. Li Y, Liu X, Chen G, Liao X. A new hyperchaotic Lorenz-type system: generation, analysis, and implementation. *Int J Circ Theor Appl*. 2011;39:865-879.
29. Cannas B, Cincotti S. Hyperchaotic behaviour of two bi-directionally coupled Chua's circuits. *Int J Circ Theor Appl*. 2002;30(6):625-637.
30. Li Q, Yang X. Hyperchaos from two coupled Wien-bridge oscillators. *Int J Circ Theor Appl*. 2008;36(1):19-29.
31. Yang X, Li Q, Chen G. A twin-star hyperchaotic attractor and its circuit implementation. *Int J Circ Theor Appl*. 2003;31(6):637-640.
32. Hu G. Hyperchaos of higher order and its circuit implementation. *Int J Circ Theor Appl*. 2011;39(1):79-89.
33. Shen C, Yu S, Lü J, Chen G. Constructing hyperchaotic systems at will. *Int J Circ Theor Appl*. 2015;43(12):2039-2056.
34. Bao B, Bao H, Wang N, Chen M, Xu Q. Hidden extreme multistability in memristive hyperchaotic system. *Chaos Soliton Fract*. 2017;94:102-111.
35. Chlouverakis KE, Sprott JC. Chaotic hyperjerk systems. *Chaos Solitons Fract*. 2006;28(3):739-746.
36. Davy JL. Properties of the solution set of a generalized differential equation. *Austral Math Soc*. 1972;6(03):379-398.
37. Leonov GA, Kuznetsov NV. Hidden attractors in dynamical systems from hidden oscillations in Hilbert-Kolmogov, Aizerman, and Kalman problems to hidden chaotic attractors in Chua circuits. *Int J Bifurcation Chaos*. 2013;23(01):1330002.
38. Leonov GA, Vagaitsev VI, Kuznetsov NV. Localization of hidden Chua's attractors. *Phys Lett A*. 2011;375(23):2230-2233.
39. Kapitaniak T, Leonov GA. Multistability: uncovering hidden attractors. *Eur Phys J Spec Top*. 2015;224(8):1405-1408.
40. Dudkowski D, Jafari S, Kapitaniak T, Kuznetsov NV, Leonov GA, Prasad A. Hidden attractors in dynamical systems. *Phys Rep*. 2016;637(3):1-50.
41. Wei Z, Wang R, Liu A. A new finding of the existence of hidden hyperchaotic attractors with no equilibria. *Math Comput Simulat*. 2014;100:13-23.
42. Kuznetsov NV, Leonov GA, Mokaev TN, Prasad A, Shrimali MD. Finite-time Lyapunov dimension and hidden attractor of the Rabinovich system. *Nonlinear Dyn*. 2018;92(2):267-285.
43. Gans RF. When is cutting chaotic? *J Sound Vibr*. 1995;188(1):75-83.
44. Sun K, Sprott JC. Periodically forced chaotic system with signum nonlinearity. *Int J Bifurcat Chaos*. 2010;20(5):1499-1507.
45. Sprott JC. Symmetric time-reversible flows with a strange attractor. *Int J Bifurcation Chaos*. 2015;25(5):1550078.
46. Li C, Sprott JC. How to bridge attractors and repellors. *Int J Bifurcation Chaos*. 2017;27(10). 1750149
47. Hoover WG, Kum O, Posch HA. Time-reversible dissipative ergodic maps. *Phys Rev E*. 1996;53(3):2123-2129.
48. Li P, Zheng T, Li C, Wang X, Hu W. A unique jerk system with hidden chaotic oscillation. *Nonlinear Dyn*. 2016;86(1):197-203.
49. Tsubone T, Saito T. Hyperchaos from a 4-D manifold piecewise-linear system. *IEEE Trans on Circuits Syst—I: Fund Theor Appl*. 1998;45(9):889-894.
50. Li C, Sprott JC, Thio W, Zhu H. A new piecewise linear hyperchaotic circuit. *IEEE Trans. on Circuits Syst.—II: Exp Briefs*. 2014;61(12):977-981.
51. Li Z, Zhu X, Hu W, Jiang F. Principles of chaotic signal radar. *Int J Bifurcation Chaos*. 2007;17(05):1735-1739.
52. Hu W, Li Z, Li C, Zhu X, Jiang F. Synchronization-based scheme for calculating ambiguity functions of wideband chaotic signals. *IEEE Trans on Aerosp Electron Syst*. 2008;44(1). 9943776

How to cite this article: Li C, Akgul A, Sprott JC, Iu HHC, Thio WJ-C. A symmetric pair of hyperchaotic attractors. *Int J Circ Theor Appl*. 2018;1–10. https://doi.org/10.1002/cta.2569